#5312

AIR MOVEMENT & VENTILATION CONTROL WITHIN BUILDINGS

12th AIVC Conference, Ottawa, Canada
24-27 September, 1991

Paper No. Poster #43 (please leave blank)

Title

NUMERICAL PREDICTION OF VENTILATION SYSTEM PERFORMANCE IN AN OPEN OFFICE SPACE

Author (s) Jin B. Fang and Andrew Persily

Affiliation Building and Fire Research Laboratory
National Institute of Standards and Technology
Gaithersburg, MD 20899
USA

ABSTRACT

Numerical modeling is performed to predict airflow patterns, thermal comfort, and ventilation air distribution within an open office space. This analysis is conducted to examine the ability of a three-dimensional airflow simulation model to predict the performance of a linear diffuser and to assess the impact of several parameters on performance. The airflow within a single cubicle within a mechanically ventilated open office area is modeled numerically using the program EXACT3. The airflow patterns, temperature distributions and local age of air are calculated for different air exchange rates, interior partition locations and discharge angles of the supply air, using a three-dimensional, turbulent flow finite difference model. Thermal comfort within the space is described by the Air Diffusion Performance Index (ADPI), and ventilation effectiveness is determined with a simulated tracer gas measurement of the local age of air.

1. INTRODUCTION

Building ventilation systems are designed to provide a thermally acceptable environment under varying heating and cooling loads, to provide sufficient levels of outdoor air to the occupied space, and to remove contaminants generated within the space. The thermal comfort experienced by the occupants is dependent on the temperature, relative humidity, air speed and turbulence level within the space. The ability of the ventilation system to supply adequate levels of outdoor air and to control indoor contaminants depends on the outdoor air intake rate and the air distribution characteristics of the ventilation system. Both air speed and temperature profiles within the space and the air distribution characteristics are determined by the shape and size of the ventilated space, the configuration of the supply and return air vents, the thermal loads within the space, the ventilation flow rates, the supply vent discharge characteristics, and the presence of obstacles such as furniture.

Given the wide range of ventilation air distribution system configurations and conditions within the occupied space, the prediction of thermal comfort and air distribution performance for any specific situation is problematic. Reliable methodology has not yet been developed to predict thermal comfort and air distribution characteristics of ventilated spaces or to estimate local contaminant concentrations. Full-scale measurements are sometimes used to evaluate thermal comfort for relatively simple configurations, primarily for evaluating air distribution equipment. Such full-scale testing is expensive and time consuming, and cannot be used in the wide variety of configurations of interest. Reduced-scale models are sometimes used to provide performance information, but it is difficult to fulfill all similarity conditions. Three-dimensional, numerical simulation offers the ability to predict ventilation

characteristics over a range of operation parameters and physical configurations. Due to rapid advances in computer technology, numerical simulations are gradually being recognized as a cost effective option for evaluating the performance of building ventilation systems.

Most of the numerical modeling of air movement in building spaces is performed by application of computational fluid dynamics techniques. Murakami and Kato [1] reviewed various numerical and experimental methods used for analyzing airflow fields and contaminant distribution in rooms. They confirmed that a two-equation turbulence model was generally acceptable for three-dimensional flow simulation. Other recent work has demonstrated the usefulness of these models for studying room air motion and their ability to achieve reasonable agreement with experimental data [2-6].

Many of the previous efforts to model room air motion in ventilated spaces have involved ventilation systems with supply vents that discharge normal to the wall or ceiling of the space. While this type of supply vent does exist, it is not commonly used in North American office buildings. The ventilation systems in these buildings generally employ air diffusion systems in which the supply diffuser discharges the conditionied air at and parallel to the ceiling [7-8]. The supply air then induces room air, mixing the supply air and room air above the occupied space. This approach protects the occupants from the cold supply air (in cooling applications), and results in acceptably low air speeds and uniform temperatures within the space. When the system is well designed, with properly selected diffusers, the air within the space should be relatively well mixed. In this paper, the airflow field and air temperature distribution are predicted numerically in an open office space with an induction air distribution system. Previous work has presented such predictions for the same office space with a concentrated heat load and predicted both good thermal comfort and good ventilation effectiveness [9]. This paper reports on additional analyses for several different ventilation system and office space configurations.

2. DESCRIPTION OF COMPUTER PROGRAM

A three-dimensional finite difference computer code EXACT3 developed at NIST [10] was used to predict airflow and temperature fields. This computer code is based on finite difference approximations to the governing conservation equations of mass, momentum and energy, and solves for the flow field in primitive variable form. A staggered grid system is adopted where the velocity components are defined at the center of the grid surfaces, and scalars such as temperature and pressure are defined at the center of the grid volumes. The code employs a k-ϵ two-equation turbulence model, and an explicit time integration technique with a hybrid scheme in which either centered or upwind

differencing schemes are utilized for the convection and diffusion fluxes, depending on the local values of cell Peclet number. In the computer code, logarithmic or power law type wall functions for the velocity profiles are used to account for the near-wall regions. The governing equations describing conservation of mass, momentum, energy and turbulent kinetic energy and its dissipation rate, for a transient, three-dimensional buoyancy-driven flow under the Boussinesq approximation are presented in Fang and Persily [9]. After EXACT3 is used to calculate the three-dimensional velocity and temperature fields, its companion program CONTAM3 is used to calculate the contaminant concentration profile. A contaminant source is specified and CONTAM3 calculates the dispersal of the contaminant over time based on the flow field determined with EXACT3.

3. OFFICE CONFIGURATION AND CALCULATION PROCEDURE

The calculations discussed here concern a cubicle in an air-conditioned, open office in the interior of a building. This office module is 3.05 m by 4.88 m with a ceiling height of 2.74 m (10 ft by 16 ft by 9 ft). Figure 1 depicts a schematic of the cubicle. The thermal loads consist of the lighting loads in the ceiling and constant heat gains from office machines and building occupants, which are combined into a concentrated heat load at the center of the floor. The lighting loads consist of four recessed fluorescent light troffers. Eighty percent of the lighting load is assumed to be transported downward into the office space by convection and radiation. The office is maintained at a constant average air temperature of 23.9° C (75° F) by controlling the supply airflow rate. A linear diffuser located at the center of the ceiling delivers cold air along the ceiling through two, opposing horizontal discharge slots, each with an active length of 1.22 m (4 ft). The equivalent diameter of the diffuser nozzle, defined as four times the cross-sectional area divided by the wetted perimeter, is used as the characteristic length of the air diffuser and is equal to 6.35 mm (0.25 in). The return air is exhausted through openings at the sides of the ceiling light fixtures. Each return opening is 25 mm (1 in) wide by 1.22 m (4 ft) long. Under cooling conditions, the heat gains from the lighting loads and the concentrated heat load are offset by the supply air, which is introduced into the office at 12.8 °C (55 °F).

The numerical computation is performed on half of the cubicle employing the symmetry of the space. The half-portion of the office cubicle is subdivided non-uniformly into 27 x 20 x 27 rectangular parallelpiped cells. To better represent air motion in areas with relatively high velocity gradients, finer grid spacing is employed in the vicinity of the walls, the heat loads, and the supply and exhaust openings. All surfaces are assumed to be adiabatic except the exposed surfaces of the ceiling lights and the top portion of the concentrated load, where constant heat output rates are known. The heat inputs into the flow domain are assumed to be transmitted to the surrounding fluid cells

immediately adjacent to the heated surfaces by adding corresponding heat source terms in the energy equations.

Once the velocity and temperature fields have been calculated with EXACT3, the companion computer code CONTAM3 is used to predict the concentration buildup in the space in response to a constant injection of tracer gas into the supply air duct. These calculations are intended to simulate tracer gas measurements of ventilation effectiveness. The time variations of concentration distribution of tracer gas are calculated using the conservation equation for chemical species. Some difficulties were encountered in these calculations due to the fine grids employed in the regions near the inlet and exhaust. Because of these small grid spacings, extremely small time steps were needed to obtain a convergent solution. Coarser grids with flow velocities interpolated from local air velocity profiles were utilized to substitute for these fine grids. Calculations of the gas concentrations were carried out with a 25 x 20 x 21 nonuniform grid. The diffusion coefficient of the tracer gas is based on of sulfur hexafluoride (SF_6) diffusing in air and is estimated from the empirical correlation developed by Fuller, Schettler and Giddings [11-12]. The values for SF_6 were used due to its common use in tracer gas studies of building ventilation. This diffusion coefficient is estimated to be 0.0927 cm^2/s at one atmospheric pressure and 23.9 °C (75 °F). The Schmidt number, $Sc = \mu/\rho D$, in which μ is the viscosity, ρ is the density and D is the diffusion coefficient of tracer gas (SF_6), has a value of 0.27.

In the previous analysis of this ventilated office [9], three cases were studied corresponding to three different thermal loads. As mentioned earlier, the thermal loads in this space include a concentrated heat load at the center of the floor and lighting loads in the ceiling. Three levels of the concentrated load were used, 510, 570 and 830 W, corresponding to 34.3, 38.7 and 55.9 W/m^2 (3.19, 3.56 and 5.19 W/ft^2). The lighting loads for the three cases were 10.8, 16.2 and 16.2 W/m^2 (1.0, 1.5 and 1.5 W/ft^2). Eighty percent of the lighting loads were assumed to enter the ventilated space, with the remainder being removed with the return air. Because the average space temperature and the supply air temperature were assumed to be constant, the supply airflow rate was varied in the three cases to maintain an energy balance. The supply airflow rate in the low, medium and high load cases was 0.046, 0.055 and 0.074 m^3/s (98, 116 and 156 cfm) respectively, corresponding to 11.2, 13.3 and 17.8 $m^3/hr\text{-}m^2$ (0.61, 0.73 and 0.98 cfm/ft^2). The results of these numerical simulations indicated good thermal comfort and good ventilation effectiveness in all three cases. The analysis that follows includes simulations of the same office space with different thermal loads, modifications in the supply air discharge characteristics and the inclusion of partitions to determine how these factors affect thermal comfort and ventilation effectiveness.

4. TEST CASES AND ANALYSIS

In order to investigate the effect of selected ventilation and space parameters on thermal comfort and ventilation effectiveness, several new cases were analyzed. These test cases include lower supply airflow rates, changes in the supply airflow discharge direction and the inclusion of partitions. Table 1 shows the input parameters for the low supply airflow rate cases. These were included to see if these low supply flows degraded the ventilation system performance. It is sometimes thought that low supply airflow rates, particularly when variable air volume systems are operating under low loads, may cause supply air to "dump" or fall vertically from the diffuser rather than flow along the ceiling as intended. Such dumping can severely degrade thermal comfort within the space. The very-low case corresponds to a situation where the supply airflow rate is equal to the minimum ventilation requirement in ASHRAE Standard 62-1989 [13]. In order to maintain the energy balance in the space, the thermal loads in the space have to be drastically reduced in the very-low and medium-low cases. Otherwise, the interior air temperature would increase to an unrealistically high level. The low case in Table 1 is the low thermal load case analyzed previously [9].

The ventilation system being modelled in this office employs an induction type diffuser in which a high speed, horizontal jet is discharged at the ceiling and induces room air into the jet. Due to poor diffuser design or selection, or to inappropriate velocity profiles upstream of the diffuser, the actual supply air discharge may be other than parallel to the ceiling. Such a nonhorizontal discharge direction can interfere with the intended airflow patterns in the space, degrading thermal comfort. As shown in Table 2, four discharge angles were investigated, 10°, 30°, 45° and 60° from the ceiling. The horizontal case, included as a reference, is the medium thermal load case from the earlier analysis [9].

Another series of test cases were included to examine the effects of partitions on space air distribution. These were all done under the so-called medium thermal load. In the first case, a 1.8 m (6 ft) high partition is located at the edge of the cubicle, directly below the return vent. In the other two cases, the partition is located between the supply diffuser and the return vent. In one case the diffuser extends all the way down to the floor, while in the other case the partition is raised 0.15 m (6 in) from the floor.

4.1 THERMAL COMFORT

For each test case, the calculated air velocity field and temperature distribution were used to determine the thermal comfort performance of the air diffuser. The Air Diffusion Performance Index (ADPI) is commonly used to specify the performance of an air diffusion system and is defined as the percentage of the locations in the occupied zone that meet

acceptable limits of effective draft temperature ranging between -1.7 °C and +1.1 °C (-3 °F and 2 °F) and local air velocity of less than 0.35 m/s (70 fpm) [7]. The effective draft temperature ϕ can be calculated from the equation below:

$$\phi = (T_x - T_c) - 8.0(V_x - 0.15)$$

where T_x is the local air temperature in °C, T_c is the average room temperature in °C, and V_x is the local air velocity in m/s. The ADPI values are derived based on predicted local air temperatures and flow velocities at 150 locations distributed in the occupied zone. These locations are all within specified distances from the floor, ceiling, sides of the cubicle and the concentrated load. The thermal comfort within the occupied space is also characterized by the maximum and minimum air temperatures and the average air speed.

4.2 VENTILATION EFFECTIVENESS

In order to characterize the distribution of the supply air, a tracer gas measurement of ventilation effectiveness was simulated numerically using the calculated velocity fields. The spatial distributions of tracer gas concentrations in response to a constant injection of tracer gas (SF_6) into the supply air stream were calculated as a function of time using CONTAM3, the companion program to EXACT3. In these simulations, a unit concentration of tracer gas was injected into the supply airstream and the tracer gas concentration buildup was predicted at each location in the space. These calculated concentration profiles as a function of time were then used to calculate the average age of air at each location in the space. The average age of air, based on age distribution theory, is one of the more promising approaches used to quantify the ability of the air distribution system to deliver ventilation air to the occupants [14]. Based on a constant tracer gas injection, the local age of air at a specific location is defined by the following equation :

$$\tau_i = \int_0^\infty (1 - C_i(t)/C_{is})\, dt$$

where C_i (t) is the tracer gas concentration at location i at time t, and C_{is} is the equilibrium concentration of tracer gas at location i. C_{is} is the same throughout the space and equal to 1.0. Numerical integration of the predicted gas concentrations was performed using the trapezoidal rule with a 2-minute time step over a one hour period. The residual area, corresponding to the "tail" of the concentration versus time curve after the one hour integration interval, was estimated from the gas concentration at one hour and the slope of the logarithm of the concentration over the last 10 minutes of the buildup. Based on the time history of tracer gas concentration in the exhaust air, the average age of air in the ventilated space can be calculated from the equation below:

$$[\tau] = (1/\tau_n) \int_0^\infty (1 - C_e(t)/C_{is})\ t\ dt$$

where τ_n is the average age of air leaving the ventilated space. τ_n is equal to the volume of the space divided by the volumetric flow rate of the supply air (the air change rate of the space) and $C_e(t)$ is the gas concentration in the exhaust air.

The local air exchange effectiveness quantifies the air distribution characteristics at a specific location and is defined by the following expression:

$$\epsilon_i = \tau_n/\tau_i$$

The mean air exchange effectiveness is a measure of the overall air distribution pattern for a ventilated space and is defined by:

$$\eta = \tau_n/[\tau]$$

If the air within the space is perfectly mixed, then the local age of air τ_i will be the same throughout the space and equal to the inverse of the air change rate, i.e., τ_n. Similarly, the value of $[\tau]$ will also equal τ_n. The local air exchange effectiveness ϵ_i at all locations in the space and the mean air exchange effectiveness η will equal 1.0. In the idealized case of pure piston flow through the space, not realistic for ceiling mounted supplies and returns, τ_i will be minimized near the supply and maximized near the return. The mean age of air $[\tau]$ will be exactly equal to $\tau_n/2$, and therefore η will equal 2, its maximum possible value. The local air exchange effectiveness ϵ_i will be below 1 near the return and well above 1 near the supply. If there is non-uniform air distribution within a space, those locations with poor ventilation air distribution will have local ages of air that are higher than the space average. Locations in so-called "stagnant" regions will have values of τ_i that are relatively large and values of ϵ_i significantly less than 1, a generally undesirable situation. The existence of significant stagnation in a space will result in a value of η for the space that is well below 1.

5. RESULTS

This section presents the results for the ventilation system and room configurations discussed above. The analysis is the same as that done in the three reference cases, low, medium and high thermal loads, presented earlier [9]. Since both the calculated thermal comfort and ventilation effectiveness were good for these three cases, they serve as a reference for the comparison of the new results. The new cases were specifically selected to investigate how supply airflow rate, supply flow discharge direction and partitions might degrade thermal comfort and ventilation effectiveness.

Figure 2 shows the calculated velocity profile for the medium thermal load case in the plane that intersects the concentrated load. A turbulent cool air jet emerges horizontally from the diffuser, spreads along the ceiling while entraining the surrounding air. The flow then deflects downward at the symmetry plane opposite the inlet and turns horizontally after impinging on the floor. The flow follows the surface of the concentrated heat load, travelling upward, and entrains into the stream discharging from the diffuser. A recirculating flow structure, with its center located near the top corner formed between the ceiling and the symmetry plane opposite the inlet is observed. This is a fairly typical and expected pattern for such a ventilation system configuration. The entrainment of room air into the supply airstream prevents the cool supply air from flowing directly on the occupants and maintains a comfortable level of air motion with the space.

The thermal comfort results for the low supply airflow rate cases, referred to as very-low and medium-low, are presented in Table 3 along with the results from the low thermal load case presented in reference [9]. These cases were examined to determine the effects of these low flow rates on the diffusers ability to maintain thermal comfort in the space and to induce good mixing of the supply air with the room air. As seen in Table 1, the discharge velocities in these two cases are much lower than in the low thermal load case. One might expect low discharge velocities to decrease the ability of the supply air jet to entrain room air, potentially resulting in the dumping of supply air. The results in Table 3 indicate fairly high ADPI values for both the very-low and medium-low cases. In both cases, all of the points outside of the desired range are in the stagnant hot regime.

Table 4 shows the thermal comfort results for the different directions of supply air discharge. While diffusers are designed to discharge horizontally, in some cases the discharge direction will be affected by poor diffuser selection or inappropriate velocity profiles upstream of the diffuser. Inappropriate velocity profiles can occur because of insufficiently long and straight duct runs upstream of the diffuser. A nonhorizontal supply air discharge will degrade the entrainment of room air by the supply airstream and may result in dumping of the cool supply air directly into the occupied space. The results in Table 4 indicate lower values of ADPI with larger values of the discharge angle from horizontal. The degradations in thermal comfort are not too severe for angles between 10° and 45°, but are quite significant for 60°. In the 60° case, almost all of the points out of the optimal range are in the stagnant hot regime, with no points in the drafty regime.

Figure 3 shows the calculated velocity profile for the 60° supply air discharge case. The supply airflow is seen to drop from the diffuser and sweep to the right of the concentrated load. A two-cell circulation pattern develops in the room. Only selected points within the occupied space were used to calculate ADPI,

resulting in a lack of cold, drafty points in Table 4. While for all other discharge angles the supply airflow stays on the ceiling, this case clearly results in dumping of the supply air.

Figures 4 and 5 show the velocity profiles for the cases in which the partition extends all the way down to the floor and in which there is some clearance under the partition. Locating the partition between the supply and return vents disrupts the overall circulation pattern in the space is seen in Figure 2. The existence of the clearance allows a significant amount of airflow under the partition as seen in Figure 5, and the circulation pattern is partially restored. The thermal comfort results for the partition cases, shown in Table 5, indicate little change in ADPI between the case with no partition and the partition located at the room edge. This partition location affects the airflow patterns very little because it is at the boundary of the overall circulation pattern seen in Figure 2. When the partition is located between the supply and return vents, and extends all the way down to the floor, the ADPI value is decreased significantly. When there is some clearance beneath the partition, the ADPI value increases close to its no partition value.

The results of the ventilation effectiveness analyses are shown in Tables 6 through 8. Table 6 shows the results for the low supply airflow rate cases. The mean air exchange effectiveness and the range of local air exchange effectiveness for both the very-low and medium-low cases are very similar. The are both slightly less than the perfect mixing value of 1.0, and less than the low thermal load case. But even in these very low airflow situations, the supply air is mixing the room air quite well as intended.

Table 7 shows the ventilation effectiveness results for the different directions of supply air discharge. The nonhorizontal discharge cases deviate somewhat from the reference case of horizontal discharge and from the idealized case of perfect mixing. The deviations in the mean air exchange effectiveness are all less than 10% except in the 45° case. The local air exchange effectiveness values get fairly low in both the 45° and the 60° cases.

Table 8 shows the ventilation effectiveness results for the partition cases, with the no partition, medium load case shown as the reference. As in the case of thermal comfort, locating the partition under the return vent has little effect on the ventilation effectiveness. When the partition is located between the supply and return, the effect is more significant. When the partition extends to the floor, it disrupts the overall circulation pattern and the mean air exchange effectiveness drops to 0.61. The local values range from 0.56 to 0.71, indicating poor mixing of the supply air within the occupied zone. When clearance is provided under the partition, the supply air mixing improves significantly. The mean air exchange effectiveness increases to 0.89 and the minimum local value is only 0.84.

6. CONCLUSIONS

The flow fields, air temperature distributions and contaminant concentrations were predicted numerically in a mechanically ventilated open office for different supply airflow rates, partition locations, and supply air discharge angles. Thermal comfort, in terms of the ADPI (Air Diffusion Performance Index), and ventilation effectiveness, in terms of the age of air, are calculated and compared for each case. The low supply airflow rates did not degrade either thermal comfort or ventilation effectiveness significantly, but that is due in part to the low thermal loads employed in these cases. Low loads were used to prevent overheating of the space, and made it easier to achieve good thermal comfort. The supply air discharge angle was not found to significantly affect thermal comfort or ventilation effectiveness until it was over 45° from horizontal. When the angle was 45° or less, the supply airflow tended to reattach to the ceiling, and good induction of the room air was achieved. When the angle was 60°, the supply air flowed into the space, degrading thermal comfort. The calculated ventilation effectiveness was not significantly affected by the discharge angle. Positioning a partition at the edge of the cubicle, under the return vent, did not significantly change the airflow pattern within the space, and therefore the calculated thermal comfort and ventilation effectiveness were not affected. Locating the partition between the supply and return vents did disrupt the airflow pattern and degraded both thermal comfort and ventilation effectiveness. Providing clearance under the partition partially restored the airflow pattern, improving both the ADPI and ventilation effectiveness. All of these results, particularly those for the different supply air discharge angles are very dependent on the boundary conditions, particularly those at the diffuser. Specifying the boundary conditions at the diffuser remain one of the challanges of three-dimensional modeling of mechanically ventilated spaces. Along with this additional work on diffuser modeling, experimental data are needed to verify these predicted results. As progress continues, numerical calculation procedures will play an increasing part in designing ventilation systems and developing strategies for healthy buildings.

7. ACKNOWLEDGEMENTS

This work was supported by the U. S. Department of Energy, Office of Building Energy Research, Conservation and Renewable Energy through an interagency agreement with the National Institute of Standards and Technology.

8. REFERENCES

1. Murakami, S. and S. Kato. 1989. "Current Status of Numerical and Experimental Methods for Analyzing Flow Field and Diffusion Field in a Room." in Christianson, L. L. (ed.), Building Systems: Room Air and Air Contaminant Distribution, ASHRAE, Atlanta, GA.

2. Davidson, L. and E. Olsson. 1987. "Calculation of Age and Local Purging Flow Rate in Rooms." Building and Environment, Vol.22.

3. Kurabuchi, T., Y. Sakamoto and M. Kaizuka. 1989. "Numerical Prediction of Indoor Airflows by Means of the K-e Turbulence Model." in Christianson, L. L. (ed.), Building Systems: Room Air and Air Contaminant Distribution, ASHRAE, Atlanta, GA.

4. Choi, H.L. and L.D. Albright. 1989. "Modeling Effects of Obstructions in Slot-Ventilated Enclosures." in Christanson, L. L. (ed.), Building Systems: Room Air and Air Contaminant Distribution, ASHRAE, Atlanta, GA.

5. Fang, J.B., R.A. Grot, 1990 "Numerical Simulation of the Performance of Building Ventilation Systems," ASHRAE Transactions, Vol.96, Part 2.

6. Haghighat, F., J.C.Y. Wang and Z. Jiang. 1990. "Three-Dimensional Analysis of Airflow Pattern and Contaminant Disperson in a Ventilated Two-Zone Enclosure." ASHRAE Transactions, Vol.96, Part 1.

7. ASHRAE. 1989. ASHRAE Handbook of Fundamentals. American Society of Heating, Refrigerating, and Air-Conditioning Engineers, Inc., Atlanta, GA.

8. Nevins, R. 1974. Air Diffusion Dynamics. Business News Publishing, Birmingham, Michigan.

9. Fang, J.B., A.K. Persily, 1991. "Numerical Prediction of Airflow Patterns and Ventilation Effectiveness in an Open Office Environment," ASHRAE Transactions, in review.

10. Kurabuchi, T., J.B. Fang, and R.A. Grot. 1990. "Numerical Method for Calculating Indoor Air Flows Using a Turbulence Model." NISTIR 90-4211.

11. Fuller, E.N., P.D. Schettler, and J.C. Giddings. 1966. "A New Method for Prediction of Binary Gas-Phase Diffusion Coefficients." Industrial and Engineering Chemistry, Vol.58.

12. Reid, R.C., J.M. Prausnitz, and T.K. Sherwood. 1977. The Properties of Gases and Liquids. Third Edition, McGraw-Hill Book Co., New York, NY.

13. ASHRAE. 1989. Standard 62-1989, "Ventilation for Acceptable Indoor Air Quality." American Society of Heating, Refrigerating and Air-Conditioning Engineers, Inc. Atlanta, GA.

14. Sandberg, M. 1983. "Ventilation Efficiency as a Guide to Design." ASHRAE Transactions, Vol.89, Part 2.

Table 1 Input Parameters for Low Airflow Rate Cases

	Air Supply Rate		
	Very-Low	Medium-Low	Low
Cooling Load (W/m^2)	14.0	26.9	43.1
(W/ft^2)	(1.3)	(2.5)	(4.0)
Air Supply Rate ($m^3/h\text{-}m^2$)	3.66	7.02	11.2
(cfm/ft^2)	(0.20)	(0.38)	(0.61)
Discharge Velocity (m/s)	1.95	3.72	5.97
(fpm)	(384)	(732)	(1176)
Reynolds Number	860	1640	2630
Archimedes Number	6.1×10^{-4}	1.7×10^{-4}	6.5×10^{-5}
Air Change Rate (1/h)	1.33	2.54	4.08

Table 2 Input Parameters for Supply Airflow Direction Cases

	Discharge Angle				
	Horizontal	10-degree	30-degree	45-degree	60-degree
Discharge Velocity :					
Horizontal (m/s)	7.07	6.97	6.12	5.00	3.54
(fpm)	(1390)	(1370)	(1210)	(980)	(700)
Vertical (m/s)	0	1.23	3.54	5.00	6.12
(fpm)		(240)	(700)	(980)	(1210)
Reynolds #	3110	3070	2700	2200	2700
Archimedes #	4.7×10^{-5}	4.8×10^{-5}	6.2×10^{-5}	9.3×10^{-5}	6.2×10^{-5}

Note: The supply airflow rate used in these cases is 13.26 $m^3/h\text{-}m^2$ (0.725 cfm/ft^2) of floor area, with a heating load of 51.13 W/m^2 (4.75 W/ft^2) and an air change rate of 4.83 per hour.

Table 3 Thermal Comfort Results for Low Airflow Rate Cases

	Air Supply Rate		
	Very-Low	Medium-Low	Low
ADPI Value	91.3	96.0	96.0
Drafty (%)			
V> 0.35 m/s	0.0	0.0	0.0
Stagnant Cold (%)			
$\Delta T > -2.8$ °C			
$\phi < -1.7$ °C			
V < 0.35 m/s	0.0	0.0	1.3
Stagnant Hot (%)			
$\Delta T < 2.8$ °C			
$\phi > 1.1$ °C			
V < 0.35 m/s	8.7	4.0	2.7
Air Temperatures (°C)			
Maximum	24.4	25.1	25.7
Minimum	23.0	23.0	22.8
Average Air Velocity			
(m/s)	0.046	0.068	0.090
(fpm)	(9.1)	(13.4)	(17.7)

Table 4 Thermal Comfort Results for Supply Airflow Direction Cases

	Discharge Angle				
	Horizontal	10-degree	30-degree	45-degree	60-degree
ADPI Value	90.7	89.3	88.7	87.3	60.0
Drafty (%)	0.7	0.0	0.0	0.0	0.0
Stagnant Cold (%)	2.0	4.0	4.7	2.0	0.0
Stagnant Hot (%)	0.7	6.7	6.7	10.7	40.0
Air Temperatures (°C)					
Maximum	25.9	25.8	25.9	26.0	25.2
Minimum	22.6	22.6	22.5	22.1	22.3
Average Air Velocity					
(m/s)	0.096	0.100	0.089	0.080	0.040
(fpm)	(18.9)	(19.7)	(17.5)	(15.7)	(7.9)

Please type ASHRAE number this at bottom

Table 5 Thermal Comfort Results for Partition Cases

		Partition		
	No Partition	Room Edge	Center No Clearance	Center Clearance
ADPI Value	90.7	90.7	79.3	88.0
Drafty (%)	0.7	0.0	0.0	0.0
Stagnant Cold (%)	2.0	1.3	4.0	6.7
Stagnant Hot (%)	6.7	8.0	16.7	5.3
Air Temperatures (°C)				
Maximum	25.9	25.8	26.3	26.1
Minimum	22.6	22.5	22.4	22.4
Average Air Velocity				
(m/s)	0.096	0.084	0.080	0.087
(fpm)	(18.9)	(16.5)	(15.7)	(17.1)

Table 6 Ventilation Effectiveness Results for Low Airflow Rate Cases

	Air Supply Rate		
	Very-Low	Medium-Low	Low
Average Age of Interior Air, $[\tau]$ (min)	48.2	25.1	11.9
Local Mean Age of Air, τ_i (min)			
Maximum	49.3	25.7	12.5
Minimum	45.1	23.4	11.3
Age of Air Leaving the Space, τ_η (min)	45.0	23.6	12.4
Mean Air Exchange Effectiveness, η	0.93	0.94	1.04
Local Air Exchange Effectiveness, ϵ_i			
Maximum	1.00	1.01	1.10
Minimum	0.91	0.92	0.99

Table 7 Ventilation Effectiveness Results for Supply Airflow Direction Cases

	Discharge Angle				
	Horizontal	10-Degree	30-Degree	45-Degree	60-Degree
Average Age of Interior Air, $[\tau]$ (min)	12.5	11.7	11.8	14.1	13.4
Local Mean Age of Air, τ_i (min)					
Maximum	13.1	12.4	12.6	15.5	17.5
Minimum	11.8	11.1	11.1	13.2	11.6
Mean Air Exchange Effectiveness, η	0.99	1.06	1.05	0.88	0.93
Local Air Exchange Effectiveness, ϵ_i					
Maximum	1.05	1.12	1.12	0.94	1.08
Minimum	0.95	1.01	0.99	0.80	0.71

Note: All of the cases have the same supply airflow rate, and therefore they all have the same value of τ_n = 12.4 (min).

Table 8 Ventilation Effectiveness Results for Partition Cases

		Partition		
	No Partition	Room Edge	Center No Clearance	Center Clearance
Average Age of Interior Air, $[\tau]$ (min)	12.5	11.1	20.5	14.0
Local Mean Age of Air, τ_i (min)				
Maximum	13.1	11.5	22.4	14.9
Minimum	11.8	10.0	17.5	12.6
Mean Air Exchange Effectiveness, η	0.99	1.12	0.61	0.89
Local Air Exchange Effectiveness, ϵ_i				
Maximum	1.05	1.25	0.71	0.98
Minimum	0.95	1.08	0.56	0.84

Note: All of the cases have the same supply airflow rate, and therefore they all have the same value of τ_n = 12.4 (min).

Please type page number as shown

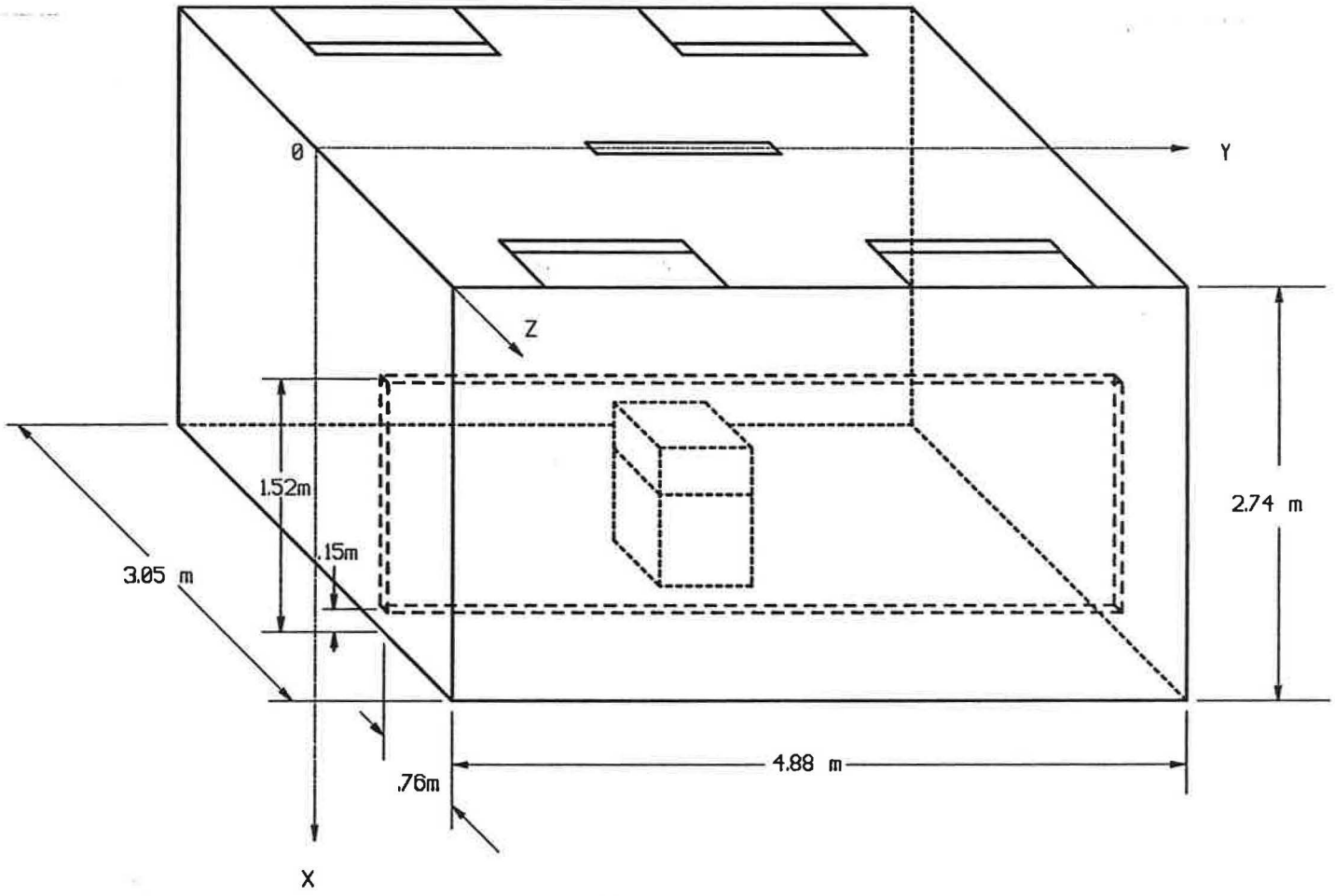

Figure 1 Schematic of Modelled Office Cubicle

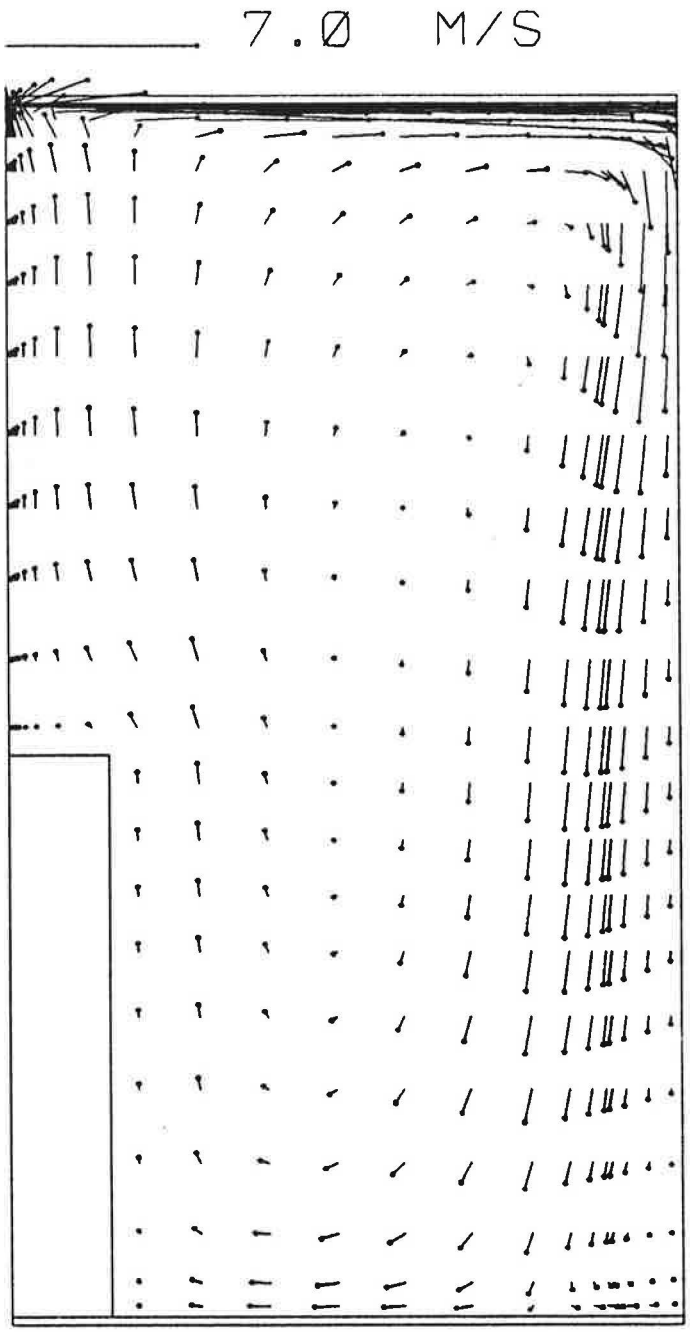

Figure 2 Calculated Velocity Vectors for the Medium Supply Airflow Rate

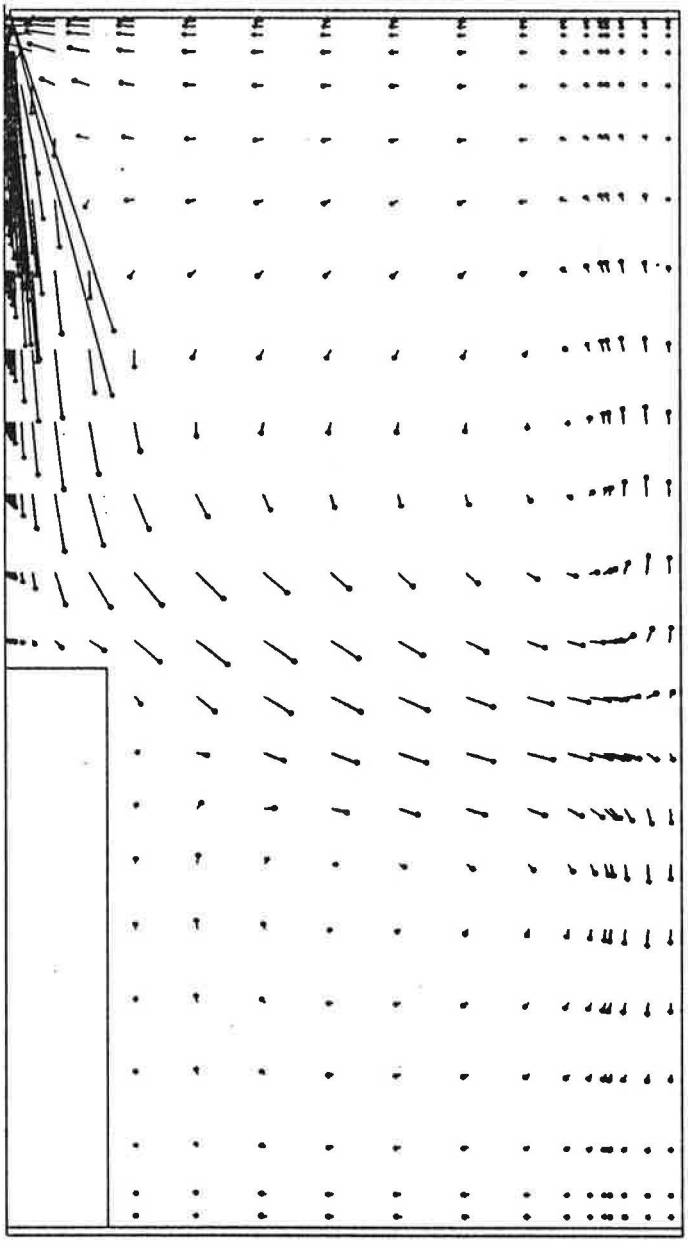

Figure 3 Calculated Velocity Vectors for 60 Degree Supply Air Discharge

Please type page number inside square

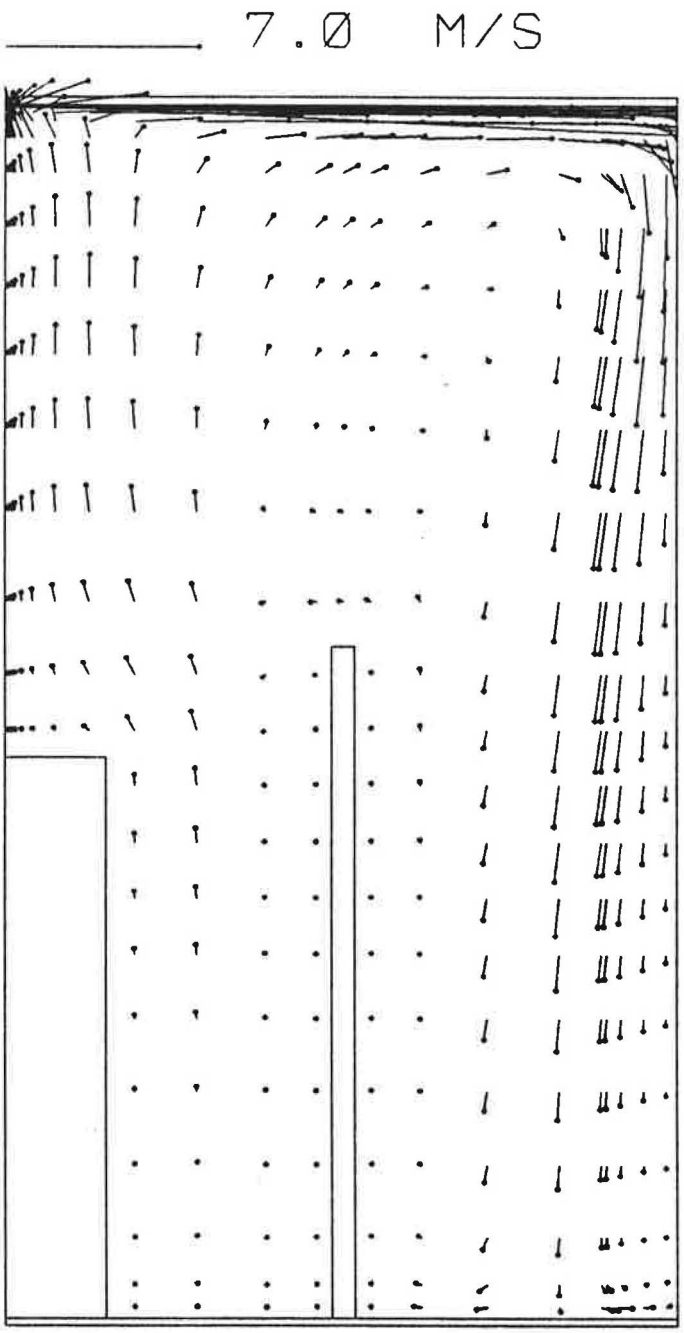

Figure 4 Calculated Velocity Vectors for the Full Length Partition Located in the Center of the Room

Please type page number or name and date

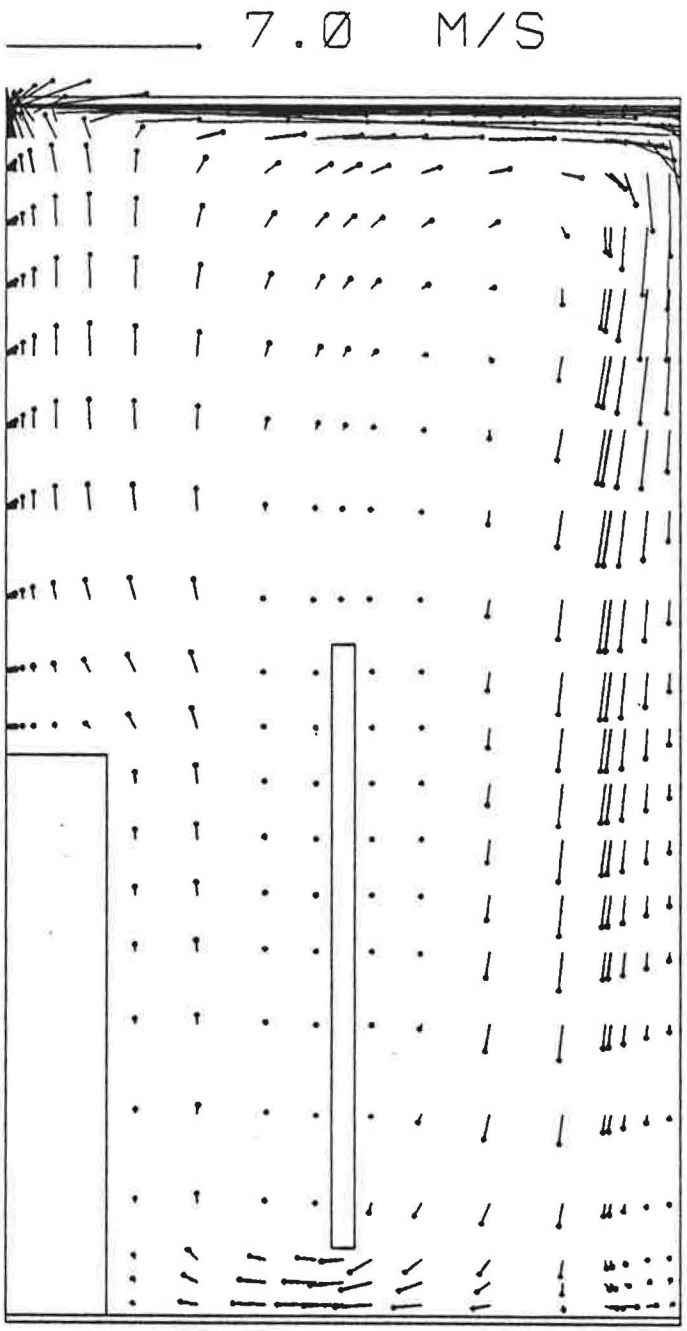

Figure 5 Calculated Velocity Vectors for the Partition with Clearance

Please type page number inside square